Fire Detection in Radiant Energy Domain for Video Surveillance

Yan Liu[1], Wei Wu[1], Zhaohui Wu[2], Zhong Zhou*[1]
[1]*State Key Laboratory of Virtual Reality Technology and Systems*
School of Computer Science and Engineering, Beihang University, Beijing, China
zz@buaa.edu.cn
[2]*China Academy of Transportation Sciences*
wzh0005@gmail.com

***Abstract*—This paper presents a novel approach of video fire detection by the features of fire extracted in radiant energy domain. Firstly, a fire color model in YCbCr color space is applied to extract fire-colored pixels as candidate regions of fire. Secondly, we convert the color space of the candidate regions into radiant energy domain through camera calibration in advance and model six features of fire with spectral irradiances to better present the physical characteristics of fire. Finally, a two-class SVM classifier with a RBF kernel is adopted to recognize fire from the candidate regions. A series of experiments have been carried out on two different datasets. Experimental results illustrate that our approach performs well when compared with other state-of-the-art methods.**

***Keywords*-fire detection; spectral irradiance; camera calibration; feature extraction; SVM classifier**

I. Introduction

Fire is one of the most harmful natural disasters and fire surveillance affects everyday life around the world. The traditional fire detection method is employing persons to inspect fire, but the human resource is expensive and inefficient for wide and complex areas. Another method is using fire sensors to detect the particles generated by fire, the temperature and relative humidity of the environment, and so on. However, these sensors are not triggered until the particles actually reach them, and usually unable to provide any additional information about the burning process, such as the location and size of fire, the degree of burning. The system manager still needs to visit the location for confirming the existence of fire when the alarm is triggered. Nowadays, surveillance cameras are installed in almost all of the public places. And the CCD video camera is considered as the most promising technology for automatic fire detection owing to its low cost, high resolution, rapid response and easy confirmation of the alarmed events through the surveillance monitor.

In the past years, video-based fire detection techniques have been extensively investigated. The main challenge in such fire detection technique is modeling the chaotic and complex nature of fire phenomenon and the large variations of fire appearance in video. Most of the existing methods use motion detection as well as color analysis to detect fire. However, many fire-colored moving objects are identified as fire, e.g., the sun, falling leaves in autumn, various artificial lights or light reflections on various surfaces, red-clothed walking people etc. Therefore, further analysis of fire motion in video is needed to get more accurate fire detection systems. A lot of researchers analyze the spatial change and temporal difference of fire by wavelet analysis, Markov Model, Fourier Transform, and so on. Some methods also incorporate dynamic texture analysis into the fire detection systems. But it is difficult to balance the detection speed and accuracy. Moreover, video quality and scene complexity also affect the robustness of vision-based fire detection algorithms.

In this paper, a novel fire detection algorithm is presented. The main contributions include: a) simplifying and validating the existing algorithm for extracting the candidate fire regions; b) modeling spectral irradiance features of fire, which can better present the physical characteristics of fire. Four state-of-the-art fire detection algorithms are compared with our method on two widely used fire detection datasets. Experiment results illustrate that our algorithm achieves a comparable detection rate with the highest frame rate.

The remainder of this paper is organized as follows: the related work and a general overview of the proposed method are presented in Section II. Section III describes the segmentation of candidate fire regions. The calculation of spectral irradiance features and classification of candidate fire regions are presented in Section IV and V respectively. Experiment evaluation is discussed in Section VI, and the conclusions are drawn in Section VII.

II. Related work

To detect fire in video, the characteristics of fire must be identified by means of modeling fire behavior. Color detection is the primary detection method in video fire detection techniques. G. Healey et al. [1] used purely color information to distinguish fire, and it is usually the first step of many other fire detection algorithms. T.Celik et al.[2] proposed a generic color model for the classification of fire pixels in YCbCr color space. The proposed model performed well in segmenting fire regions in video sequences. T.Celik et al.[3] combined color information with registered background scene to detect fire in real time.

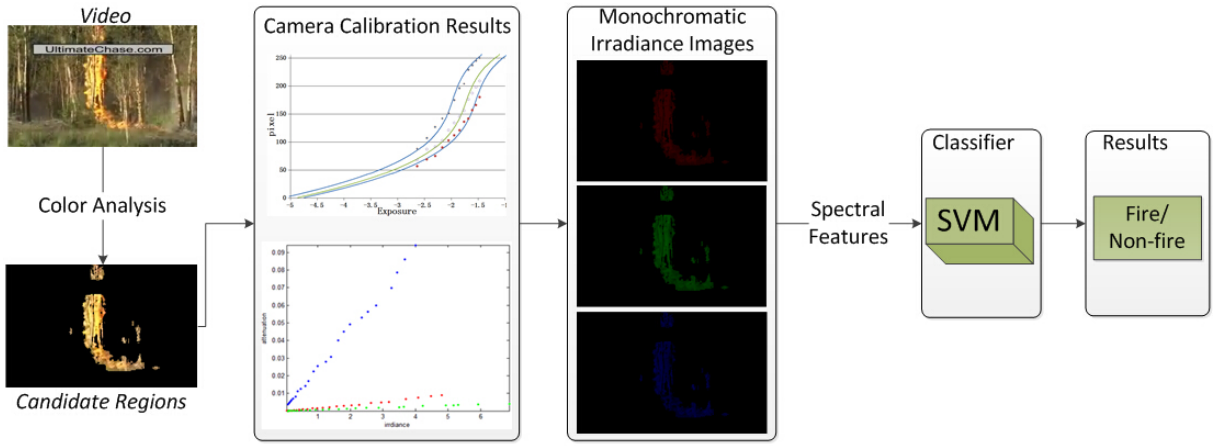

Figure 1. The process of our video fire detection algorithm.

If only color information and motion detection are used, some fire-colored moving objects are often mistakenly detected as fire. In order to get more accurate systems, further analysis of the appearance and moving characteristics of fire in video is necessary. P.V.K.Borges et al.[4] exploited some important low-level visual features of fire, including color, area size, texture, boundary roughness and skewness of the estimated fire regions. This method was applicable not only for real time fire detection, but also for video retrieval. X.Qi et al.[5] analyzed the temporal variation of fire intensities, the spatial variation of fire color and the tendency of fire to be grouped around a central point. This method was effective in detecting all types of uncontrolled fire. B. Ugur Treyin et al.[6] used a hidden Markov model to mimic the temporal behavior of fire. Specifically, the Markov model was applied to distinguish the flicker process of fire from the motion of fire-colored moving objects, and evaluate spatial variations of fire color. J.Chen et al.[7] applied multi-feature fusion to detect fire in video. It incorporated motion and color clues, as well as flicker detection.

With the development of wavelet analysis, it is widely used in detecting the spatial and temporal characteristics of fire. B. Ugur Toreyin et al.[8] detected fire flicker by analyzing the video in the wavelet domain. The algorithm used 1-D temporal wavelet transform to check the flicker of fire and analyzed the color variations in fire-colored moving regions by 2-D spatial wavelet transform. Osman Gnay et al.[9] utilized the hidden Markov model and temporal wavelet analysis to detect irregular nature of fire boundaries, and also used spatial wavelet transform to detect the color variations in fire. Different spatio-temporal features were combined in [10] to detect fire. For discriminating between fire and non-fire regions, two classification methods are investigated: a Support Vector Machine (SVM) classifier and a rule-based approach. K. Dimitropoulos et al.[11] incorporated spatio-temporal consistency energy into the algorithm [10] and raised the detection rate. Furthermore, K. Dimitropoulos et al.[12] added dynamic texture analysis to the algorithm [11]. This method was proved extremely robust to false alarms.In this paper, a novel fire detection method is proposed to extract fire features in the radiant energy domain. The process is shown in Fig 1.

As can be seen from Fig 1, firstly, the color analysis algorithm is applied to isolate candidate fire regions in each video frame. Secondly, the common surveillance camera is calibrated to restore the spectral irradiances at R, G and B wavelengths from the color images for extracting physical characteristics of fire. Thirdly, six spectral features are modeled with the spectral irradiances to improve the recognition rate. Finally, a two-class Support Vector Machines (SVM) classifier with a radial basis function (RBF) kernel is designed to detect the fire phenomenon from the candidate fire regions. These steps will be described in the following sections.

III. Segmentation of Candidate Fire Regions

In this section, color analysis is used to extract the candidate regions for each frame, because fire is obviously different from other ordinary things in its color appearance.

A. Color analysis

Although there are various kinds of fire, fire, especially at the beginning of combustion, exhibits a certain color range from red to yellow. The fire color model [13] proposed by Chen et al. was widely used in the preprocessing stage of fire detection. It was modeled in RGB color space and could exclude most of the non-fire pixels but lost fire details. As the fact that fire is a luminous body, YCbCr color space is more suitable for presenting fire than RGB color space because it is better in discriminating the luminance from the chrominance. Turgay Celik et al.[2] proposed a rule-based color model in YCbCr color space. Experiment results

showed that the YCbCr color model [2] performed well in segmenting fire regions in video sequences.

Through lots of experiments on fire and non-fire datasets, we find that the last rule of the color model [2] makes little contribution to the classification of fire pixels, but it is the most time consuming rule. Then, our method only applies the first four rules of the color model [2] to obtain the candidate regions(Fig 1, Fig 2).

Figure 2. Comparison of three moving detection algorithms. (a) a fire video; (b) our color analysis result; (c-e) the binary images of the detection results of algorithm [14][15][16] respectively.

Though many fire detection algorithms apply moving detection to help remove still pixels from the candidate regions, many details of fire will also be removed. The reason is that the motion of fire is beating and flickering in situ, while the motion of ordinary objects is changing in location. As a result, general moving detection algorithms [14][15][16] often subtract many fire pixels which change little across frames as shown in Fig 2. When fire is small, it will result in too little fire pixels in the candidate regions to successfully identify fire.

IV. Model of Spectral Irradiance Features

In this section, six spectral features of fire are modeled in radiant energy domain to eliminate fire-colored ordinary objects in candidate regions. The calculation of monochromatic irradiances and fire spectral features are described as follows.

A. Calculation of monochromatic irradiance

To restore the irradiances from color images, the camera response functions are calculated, and the spectral irradiance attenuations are calibrated to compute the monochromatic irradiances at R, G and B wavelengths.

1) Camera response function calculation: Camera response function describes the relationship between image pixel value and the irradiance accepted by CCD. Here, we adopt the method [17] to calculate the response function of

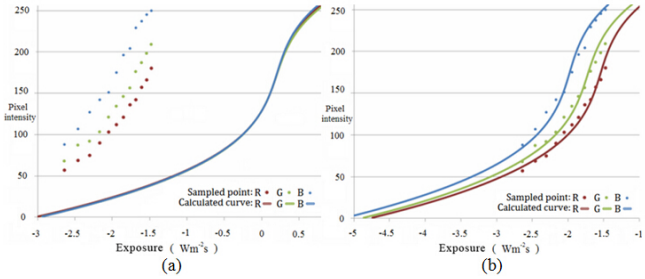

Figure 3. Response functions of camera point-grey Flea2 08S2C for R, G, B channels. (a) is the relative response functions, where ; (b) is the physical response functions, where the constant c is determined using a photometer.

our common surveillance camera. As we know, pixel values can be regarded as a function of exposure (Eq.1).

$$p_{ij} = f(E_i \cdot \Delta t_j) \tag{1}$$

where p_{ij} is the ith pixel of the jth image, f is the camera response function, E_i is the corresponding irradiance value, and Δt_j is the jth image exposure time. As the reason that the inverse function of f (denoted as f^{-1}) exists, Eq.1 can be rewritten as :

$$g(p_{ij}) = \ln f^{-1}(p_{ij}) = \ln E_i + \ln \Delta t_j \tag{2}$$

Then we can obtain the irradiance value from the corresponding pixel value, if g and Δt are known. Here, we use the multi-exposure method [17] to minimize the following quadratic objective function:

$$\begin{aligned} O = &\sum_{i=1}^{N}\sum_{j=1}^{M}\{\omega(p_{ij})[g(p_{ij}) - \ln E_i - \ln \Delta t_j]\}^2 \\ &+ \lambda \sum_{p=p_{\min}}^{p=p_{\max}} [\omega(p) g^n(p)]^2 \end{aligned} \tag{3}$$

where N is the number of pixels in an image, M is the number of images, $\omega(p)$ is the weighting function, and λ controls the smoothness of g. By solving Eq.3 with SVD, we get the relative values between the camera response function $g(p_{ij})$ and the irradiance E_j as shown in Fig 3 (a). They are regulated by a scale factor c . To determine the constant c, a photometer is used to further measure the absolute irradiance. The calibration results of our surveillance camera are shown in Fig 3 (b).

2) Irradiance attenuation calibration: The relationship between pixel value p_{ij} and irradiance E at a specific wavelength λ can be described as:

$$E_\lambda = \alpha(\lambda, p_{ij}) \cdot E_c = \alpha \cdot g(p_{ij}) \tag{4}$$

where E_c is color channel irradiance value, $g(p_{ij})$ is the logarithmic of the inverse of camera response function and α is the irradiance attenuation from the color channel E_c to the single wavelength E_λ that is decided by wavelength λ and the pixel gray level.

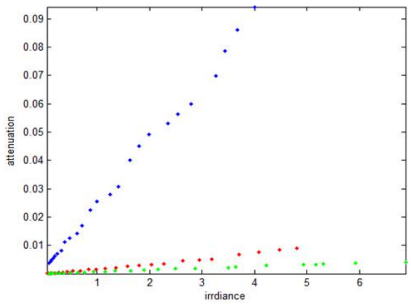

Figure 4. Irradiance attenuation at R, G, B wavelengths for our optical system.

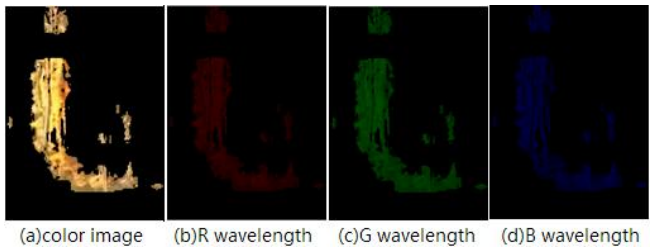

Figure 5. Calculated monochromatic images.

We also adopt the method [17] to calibrate the irradiance attenuation. Then, the irradiance attenuation at R, G and B wavelengths are calibrated for our optical system, as shown in Fig 4.

3) Monochromatic irradiance calculation: After calibration of our surveillance camera, we use the result as a universal function for common surveillance cameras because their hardware and software settings are similar. We calculate the RGB monochromatic irradiance images from the candidate fire regions of color video frame, as shown in Fig 5. Monochromatic irradiances at R, G and B wavelengths are calculated respectively for each candidate fire pixel, represented as $Er(i,j), Eg(i,j), Eb(i,j)$.

B. Extraction of spectral irradiance features

To better extract the fire features, we first divide each video frame into $N*N$ blocks. Only the blocks that contain an adequate percentage t of candidate fire pixels are selected as the candidate blocks. As shown in Fig 6, (b) is the segmented candidate fire regions of a video frame (a), and (c) is the corresponding candidate fire blocks with $N = 16, t = 30\%$. For each candidate fire block, six spectral irradiance features are modeled to represent the appearance and behavior characteristics of fire. In the following, we introduce these features in detail.

1) Models of spectral irradiance values: Human can see some kind of color because the light with the corresponding wavelength rips into eyes. The fact that fire always exhibits a color range from red to yellow illustrates that radiant energies of fire at some narrow bands follow the fixed regulars.

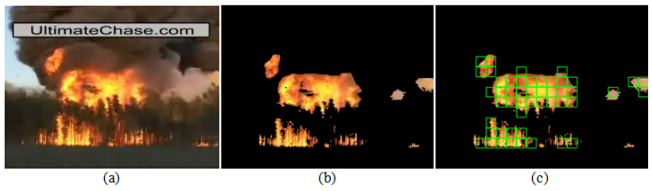

Figure 6. Candidate fire blocks of a fire video frame.

To represent the characteristics of fire appearance, we define three models in the radiant energy domain for each candidate fire block. These feature models are red spectral energy, differential spectral energy and relative spectral energy respectively. The red spectral energy is modeled as the average of the irradiance values at R wavelength of the pixels in a candidate block (Eq.5). To illustrate the difference between Er and Eb for a fire pixel, we adopt the differential spectral energy as a feature of fire defined in Eq.6. The relative spectral energy is the average of the slope of the Er-Eg curve for a candidate fire block to represent the relationship between Er and Eg (Eq.7). The following are their definitions:

$$E = \frac{1}{N}\sum_{i,j} Er(i,j) \tag{5}$$

$$D = \frac{1}{N}\sum_{i,j} |Er(i,j) - Eb(i,j)| \tag{6}$$

$$R = \frac{1}{N}\sum_{i,j} Er(i,j)/Eg(i,j) \tag{7}$$

where N is the number of candidate pixels in a block.

To show the differences of the above three features between fire candidate blocks and non-fire candidate blocks, we extract 5000 candidate blocks from four fire video sequences (Fig 7 (a)) and four non-fire video sequences (Fig 7 (b)), 2500 blocks for each type, and draw statistical histograms of these feature values for fire blocks (Fig 7 (c)) and non-fire blocks (Fig 7 (d)) respectively. From Fig 7 (c-1) and (d-1), we can see that the red spectral energy spreads between 0.1 and 0.21 when it comes to actual fire, while it varies mostly between 0.18-0.2 for non-fire blocks. The red spectral energy distribution of non-fire blocks is more concentrated maybe because the color range of fire-colored objects is limited. The differential spectral energy of fire blocks symmetrically distributes between 0.1 and 0.75, while this feature value of non-fire blocks is concentrated and spreads between 0.2 and 0.35 as shown in Fig 7 (c-2) and (d-2). Fig 7 (c-3) and (d-3) are the histograms of the relative spectral energy for fire and non-fire blocks respectively and the distributions are also different.

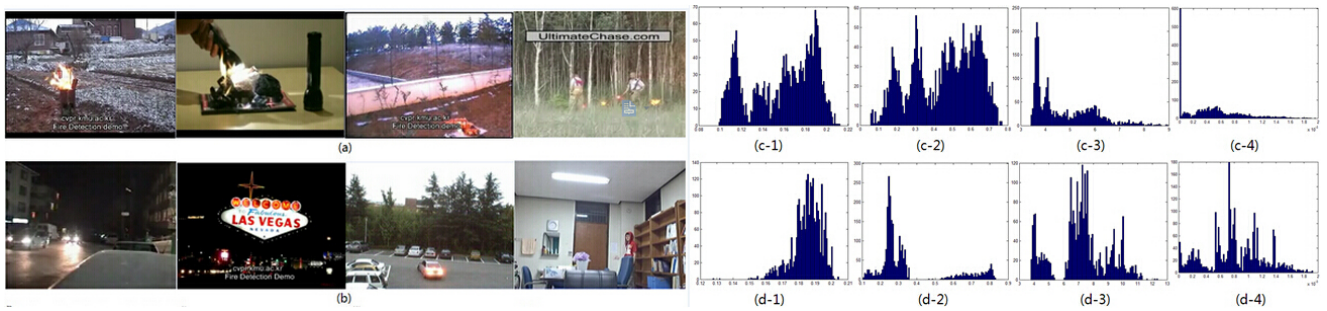

Figure 7. The statistical histograms of the extracted feature values for (a)fire candidate blocks and (b)non-fire candidate blocks. The features are red spectral energy, differential spectral energy, relative spectral energy and spectral spatial energy respectively. The row (c) is for fire blocks and the row (d) is for non-fire blocks.

2) Spectral spatial energy: Unlike other false-alarm regions, such as a red clothes, image regions containing real fire usually exhibit obviously different spatial variations because of the random nature of fire. As a result, we use the variance of the pixels' Er values as a feature of fire, we called spectral spatial energy (Eq.8), to help eliminate non-fire blocks in the candidate regions. The spectral spatial energy of each candidate fire pixel is the Er variance of itself and the pixels next to it according to the following equation:

$$Sp(i,j) = \frac{1}{K+1} \sum_{p} \sum_{q} [Er(p,q) - \overline{Er}]^2 \tag{8}$$

where K is the number of pixels next to $p(i,j)$ and (p,q) is the location of these pixels. $\overline{Er}$ is the Er mean of the pixel itself and the surrounding pixels. For each block, the spectral spatial energy is estimated as the average of the energy for the candidate pixels in the block.

$$Sp_{block} = \frac{1}{N} \sum_{i,j} Sp(i,j) \tag{9}$$

where N is the number of the candidate pixels in a block. Fig 7 (c-4) and (d-4) are histograms of this feature for fire and non-fire blocks respectively and the difference is also distinct.

3) Spectral temporal energy: One of the most notable features of fire is flickering all the time and the flicker frequency of turbulent flames is around $10Hz$ that is much more quickly than flashing lights. As a result, the radiant energy of fire changes all the time. Though the radiant energy of flashing lights also changes with time, the changing regularity of monochromatic spectral energy (we use the red spectral energy E) is obviously different because of the different traits and flickering frequency. As shown in Fig 8 (c) and (d), the red spectral energy of a fire candidate block changes gently with time, nevertheless for a non-fire candidate block containing part of a flashing light, the energy also changes with time but varies intensely.

To present the temporal characteristic of fire, the variance of the red spectral energy values through T frames is modeled as another significant feature of fire (Eq.10).

$$Te = \frac{1}{T} \sum_{t=0}^{T-1} (E_t - \overline{E})^2 \tag{10}$$

where T is the number of calculated sequence frames, $\overline{E}$ is the average of the red spectral energy E in T frames for a candidate fire block. As shown in Fig 8 (e) and (f), the spectral temporal energy varies between 0-0.0001 for a fire block, while the energy of a red flashing light block varies between 0.0002-0.012.

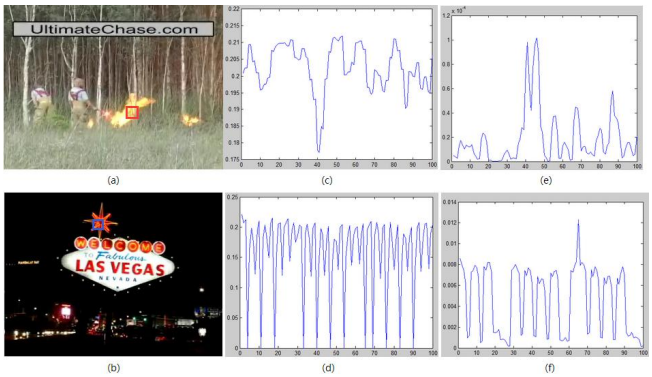

Figure 8. Changes of spectral temporal energy through 100 frames: (a) a fire block sequence; (b) a non-fire candidate block sequence; (c-d) the red spectral energy changes; (e-f) the red spectral temporal energy changes.

4) Spectral spatio-temporal energy: Due to the airflow or fire flicker, a real fire often has more spatial variations within a time interval than a fire-colored object. Unlike spectral spatial energy, which aims to identify fire spatial changes in a single frame, this feature aims to indicate the spectral spatio-temporal variations for each candidate fire block in a sequence of frames. The temporal variance of the spectral spatial energy for a candidate fire pixel within a temporal window of T last frames is:

$$ST(i,j) = \frac{1}{T+1} \sum_{t=0}^{T} (Sp_t(i,j) - \overline{Sp}(i,j))^2 \tag{11}$$

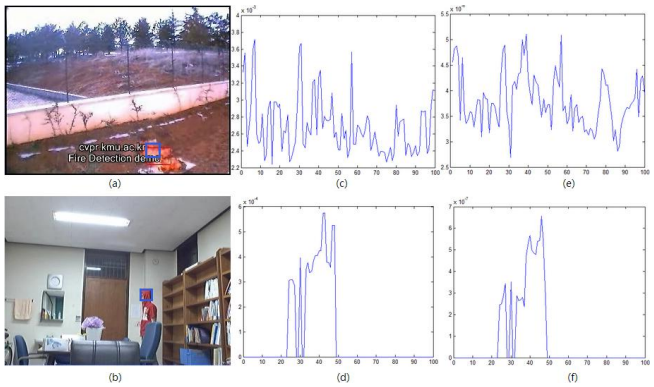

Figure 9. The spectral spatio-temporal energy changes through 100 frames. (a) a fire candidate block; (b) a non-fire candidate block. (c-d) the spectral spatial energy changes; (e-f) the spatio-temporal energy changes.

where $Sp_t(i,j)$ is the spectral spatial energy of the candidate fire pixel $p(i,j)$ in time instant t and $\overline{Sp}(i,j)$ is the average of the energy through $T+1$ frames. For each candidate block, the total spatio-temporal energy ST_{block}, is estimated by averaging the individual energy of pixels belonging to the block:

$$ST_{block} = \frac{1}{N}\sum_{i,j} ST(i,j) \tag{12}$$

To show the difference of the spectral spatial energy change between fire blocks and non-fire candidate blocks, we select two candidate blocks from a fire video and a non-fire video as shown in Fig 9 (a)(b). And their spatial energy changes through 100 frames are shown in Fig 9 (c)(d). Fig 9 (e)(f) are the corresponding spectral spatio-temporal energy changes with time. The fire block has a spatio-temporal energy between 2.7×10^{-6} and 5×10^{-6}, while the spatio-temporal energy of a non-fire candidate block is less than 6.8×10^{-7}. What's more, a fire block always has a spatio-temporal change, while a non-fire candidate block, containing part of a fire-colored moving object, presents a spatio-temporal change only in a specific time interval.

V. Classification

In order to obtain the final decision about whether a candidate block contains fire or not, classification is the last step. A feature vector consisting of six features $f = [E, D, R, Sp_{block}, Te, ST_{block}]$ is created to present the spectral feature of a candidate fire block. And a two-class (fire, non-fire) Support Vector Machines (SVM) classifier with a radial basis function (RBF) kernel is designed to classify the candidate fire blocks with the feature vector as its input. Firstly, we apply the five-fold cross validation with the training set to get the optimal values of classifier parameter c and gama. Secondly, the two-class SVM classifier with a RBF kernel is trained by the optimal parameters and the training set. Finally, we get a fire classifier model and apply it to detect fire in various videos.

Figure 10. Dataset used in Ko's experiment: Screenshots of video sequences containing (a) actual fires and (b) fire-colored moving objects.

VI. Experiment Evaluation

In this section, two datasets are used to test our method. One is Ko's dataset[19], which is widely used by [8][12][18][19]. Another is a self-collected dataset from some fire detection papers [7][10] and Internet resources. These two datasets are shown in Fig.10 and Fig.11 respectively. We employ three assessment criteria, respectively are true positive rate, false positive rate and accuracy. The true positive rate is the number of correctly detected fire frames out of the total number of fire frames. And the false positive rate is the number of non-fire frames that erroneously recognized as fire frames out of the total number of non-fire frames. The accuracy is the number of correctly detected frames out of the total number of test frames including fire and non-fire frames. For the reason of comparison with [8][12][18][19], a frame is labeled as a fire frame if it contains at least one fire block.

In each evaluation test, we follow the same training strategy for the SVM classifier, including the same training set and the same extracted features. The training set consists of 5000 randomly selected candidate blocks from four fire video sequences (Fig 10 posVideo1, posVideo2, posVideo3; Fig 11 posVideo5) and five no-fire video sequences (Fig 10 negVideo5, negVideo6, negVideo7; Fig 11 negVideo1, negVideo8). And the total number of candidate blocks are 3094, 2060, 1322, 2059 for the training fire videos and 123, 4790, 245, 109, 21 for the training non-fire videos respectively. The experiments are performed on a PC with a Core i5-3470, 3.20GHz processor and 6.00GB RAM.

A. Experiments on Ko's dataset

The video set used in Ko's experiment[19] consists of eight fire videos and eight non-fire videos(Fig 10). We test

our algorithm on them and compare with four state-of-the-art algorithms: Toreyin's algorithm[8], K.D's algorithm[12], Ko's algorithm based on hierarchical Bayesian Networks[18] and Ko's algorithm based on Fuzzy Finite Automata[19].

As shown in Tabel I, the accuracy of K.D's algorithm[12], Ko's algorithm[19] and ours are more than 99%. Toreyin's algorithm[8] produces lower detection rate than the other four algorithms because it is based purely on spatio-temporal features. In addition, Ko's method[18] produces better classification results using hierarchical Bayesian Networks, however, it also misses a significant number of real fire. Only K.D's method[12] has no false alarms. As to fire detection systems, the crucial thing is detecting fire when it happens. Our method gets the highest true positive rate than the other four algorithms. What's more, our method reaches a high frame rate, that is $41 fps$ for video sequences with resolution 320×240, and it is five times of K.D's algorithm[12]. This is because the calculation simplicity of spectral features.

Table I
COMPARISON WITH DIFFERENT METHODS.

Methods	True-Positive	False-Positive	Accuracy
ours	**99.75%**	0.71%	99.55%
Toreyin's[8]	78.9%	6.4%	88.58%
K.D's[12]	99.29%	**0.00%**	**99.6%**
Ko's[18]	93.7%	4.9%	96.75%
Ko's[19]	98.6%	0.2%	99.3%

The recognition rates on each video of Ko's dataset are shown in Table II. For fire videos, our method can all get a 100% true positive rate except video 1 and 5, because fire in some frames of these two videos is too small. The negative rates of non-fire videos are all equals to 0.00% except video 7 and 8 because some blocks of these video frames are too similar to fire.

Figure 11. Video sequences collected as another experiment dataset (a) fire videos (b) non-fire videos.

Table II
RECOGNITION RATES ON EACH VIDEO OF KO'S DATASET.

Videos	True-Positive	Videos	False-Positive
posVideo1	**98.75%**	negVideo1	0.00%
posVideo2	100%	negVideo2	0.00%
posVideo3	100%	negVideo3	0.00%
posVideo4	100%	negVideo4	0.00%
posVideo5	**99.29%**	negVideo5	0.00%
posVideo6	100%	negVideo6	0.00%
posVideo7	100%	negVideo7	**2.7%**
posVideo8	100%	negVideo8	**4.02%**

B. Experiments on other datasets

To fully prove the generality of our method, we also collected a lot of other videos from some relevant papers in fire detection and fire detection dataset websites as shown in Fig 11. PosVideo1-6 and negVideo1-2 are from the paper [10], posVideo7-8 and negVideo3 are from the paper [7]. The other videos are downloaded from http://signal.ee.bilkent.edu.tr/VisiFire/Demo/ and http:// cvpr.kmu.ac.kr/. We use the same SVM classifier as the SVM used in the experiment on Ko's dataset (Fig 10) to process these video sequences. The frame numbers of fire videos are 245, 208, 219, 246, 260, 339, 500, 140, 402 respectively, and the frame numbers of non-fire videos are 155, 1400, 244, 862, 250, 394, 102, 171, 200, 200 respectively. The recognition rate for each video sequence is given in Table III. The algorithm misses a few real fire in posVideo6 because fire in some frames is too small or fire color is too light. For posVideo7 and posVideo8, we almost have no successful detection as fire is too small. For non-fire videos, false alarms happen in negVideo2 and negVideo3 because the influence of smoke moving in front of the fire-colored background. Though there are false detections and missed detections, our method is suitable for most videos and can get a 100% true-positive rate and 0.00% false-positive rate.

Table III
RECOGNITION RATE ON EACH VIDEO OF FIG 11.

Videos	True-Positive	Videos	False-Positive
posVideo1	100%	negVideo1	0.00%
posVideo2	100%	negVideo2	**21.3%**
posVideo3	100%	negVideo3	**9.2%**
posVideo4	100%	negVideo4	0.00%
posVideo5	100%	negVideo5	0.00%
posVideo6	**99.12%**	negVideo6	0.00%
posVideo7	**1.6%**	negVideo7	0.00%
posVideo8	**0.00%**	negVideo8	0.00%
posVideo9	100%	negVideo9	0.00%
		negVideo10	0.00%

VII. Conclusion

In this paper, a novel video fire detection algorithm has been presented in radiant energy domain based on the spectral features of fire. Firstly, a fire color model in YCbCr color space was applied to isolate the candidate regions for each video frame. Secondly, we converted the color space of the candidate regions into radiant energy domain through a universal camera calibration in advance to better present the physical characteristics of fire. Thirdly, six spectral features were modeled to improve the recognition rate. Finally, a two-class SVM classifier with a RBF kernel was designed to detect fire in the candidate regions. A series of experiments have been carried out on two different datasets. Experimental results illustrated that our approach is efficient with a good fire detection rate. Furthermore, our method can be applied to real time fire detection. However, our method is difficult to detect small fire and will produce false alarms on some specific scenes. Future works will develop more distinctive features of fire and further improve the training set to reduce false alarms. Meanwhile, features of the surveillance cameras will also come into our consideration. We plan to calibrate more common surveillance cameras and integrate the calibration results. It is believed that the integrated result will produce more accurate features of fire.

Acknowledgment

This work is supported by the National 863 Program of China under Grant No.2015AA016403 and the Natural Science Foundation of China under Grant No.61472020.

References

[1] G. Healey, D. Slater, T. Lin, B. Drda, and A. D. Goedeke, A system for real-time fire detection, in IEEE Conference on Computer Vision and Pattern Recognition, June 1993.

[2] T. Celik, H. Demirel, Fire detection in video sequences using a generic color model, Fire Safety Journal (2009),147-158, doi:10.1016/j.firesaf.2008.05.005

[3] Turgay Celik , Hasan Demirel, Huseyin Ozkaramanli, Mustafa Uyguroglu,Fire detection using statistical color model in video sequences, Journal of Visual Communication and Image Representation, Volume 18, Issue 2, April 2007, Pages 176185, doi:10.1016/j.jvcir.2006.12.003

[4] Paulo Vinicius Koerich Borges, Joceli Mayer, Ebroul Izquierdo,'Efficient visual fire detection applied for video retrieval',16th European Signal Processing Conference (EUSIPCO 2008), Lausanne, Switzerland, August 25-29, 2008, copyright by EURASIP

[5] X.Qi,J.Ebert,A computer vision based method for fire detection in color videos, Int.J.Imag.2(S09)(Spring2009)2234.

[6] B. Ugur Toreyin, Yigithan Dedeoglu, A. Enis 05etin. Cetin, Flame detection in video using hidden markov models[C]// IEEE Int. Conf. On Image Proc., ICIP 2005. 2005:1230–1233.

[7] J.Chen,Y.He,J.Wang, Multi-feature fusion based fast video flame detection, Build.Environ.45(5)(May2010)11131122.

[8] B. Uur Treyin, Yigithan Dedeoglu, Ugur Gudukbay, A.Enis Cetin, Computer vision based method for real-time fire and flame detection, in Proc. IEEE Int. Conf. Image Process, 2006.Volume 27, Issue 1, 1 January 2006, Pages 4958

[9] Osman Gnay, Kasm Tademir, B. Uur Treyin, A. Enis etin, Fire Detection in Video Using LMS Based Active Learning, Fire Technology July 2010, Volume 46, Issue 3, pp 551-577, Date: 16 Sep 2009

[10] K. Dimitropoulos, F. Tsalakanidou and N. Grammalidis, "Flame detection for video-based early warning systems and 3D visualization of fire propagation," in IASTED International Conference on Computer Graphics and Imaging, 2012.

[11] P. Barmpoutis, K. Dimitropoulos and N. Grammalidis, "Real time video fire detection using spatio-temporal consistency energy," in 10th IEEE International Conference on Advanced Video and Signal-Based Surveillance, Krakow, Poland, 2013.

[12] K. Dimitropoulos, P. Barmpoutis and N. Grammalidis, Spatio-Temporal Flame Modeling and Dynamic Texture Analysis for Automatic Video-Based Fire Detection,IEEE Transactions on Circuits and Systems for Video Technology, doi: 10.1109/TCSVT.2014.2339592

[13] T. Chen, P. Wu, and Y. Chiou, An early fire-detection method based on image processing, in ICIP 04, 2004, pp. 17071710.

[14] McFarlane, N. and Schofield, C., Segmentation and tracking of piglets in images, British Machine Vision and Applications, Vol 8, pp. 187-193, 1995.

[15] Collins, R.T., Lipton, A.J., Kanade, T., A system for video surveillance and monitoring, In: Proc. American Nuclear Society (ANS) Eighth International Topical Meeting on Robotics and Remote Systems, Pittsburgh, PA, 1999.

[16] M. Van Droogenbroeck, and O. Barnich. ViBe: a disruptive method for background subtraction, In T. Bouwmans, F. Porikli, B. Hoferlin, and A. Vacavant, editors, Background Modeling and Foreground Detection for Video Surveillance, chapter 7. Chapman and Hall/CRC, pages 7.1-7.23, July 2014.

[17] Zhong Zhou, Delei Tian, Zhaohui Wu, Zhiyi Bian, Wei Wu. Three-dimensional reconstruction of flame temperature distribution using tomographic and two-color pyrometric techniques. IEEE Transactions on Instrumsentation and Measurement, 2015.

[18] B. Ko, K. Cheong and J. Nam, "Early fire detection algorithm based on irregular patterns of flames and hierarchical bayesian networks," Fire Safety Journal, vol. 45, no. 4, pp. 262-270, 2010.

[19] B. Ko, S. Ham and J. Nam, "Modeling and formalization of fuzzy finite automata for detection of irregular fire flames," IEEE Transactions on Circuits and Systems for Video Technology, vol. 21, no. 12, pp. 1903-1912, December 2011.